Oxidative activity of 17β-hydroxysteroid dehydrogenase on testosterone in male abdominal adipose tissues and cellular localization of 17β-HSD type 2

Mohamed Fouad Mansour [1], Mélissa Pelletier [1], Marie-Michèle Boulet [1,2], Dominique Mayrand [3] Gaétan Brochu [4], Stefane Lebel [2], Donald Poirier[1], Julie Fradette [3], Katherine Cianflone [2], Van Luu-The [1] and André Tchernof [1,2]

1. Endocrinology and Nephrology, CHU de Québec-Université Laval Medical Center, Québec, Canada.

2. Institut universitaire de cardiologie et de pneumologie de Québec and School of Nutrition, Université Laval, Québec, Canada.

3. Centre de recherche en organogénèse expérimentale de l'Université Laval /LOEX Division of Regenerative Medicine, CHU de Québec-Université Laval Medical Center, Québec, Canada, Department of Surgery, Université Laval, Québec, Canada

4. Department of General Surgery, CHU de Québec-Université Laval Medical Center, Québec, Canada.

Running Title: 17β-HSD type 2 activity and localization in human adipose tissue

Address for correspondence:

Andre Tchernof, Ph.D.
Endocrinology and Nephrology &
School of Nutrition
CHU de Québec-Université Laval
2705 Laurier Blvd, R-4779
Quebec City, Que
Canada G1V 4G2
Tel: 1-418-654-2296
Fax: 1-418-654-2761
Email: andre.tchernof@crchudequebec.ulaval.ca

ABSTRACT

Testosterone can be converted into androstenedione (4-dione) by 17β-hydroxysteroid dehydrogenase (HSD) activity likely performed by 17β-HSD type 2. Our objective was to evaluate the rate of testosterone conversion to 4-dione as well as expression and localization of 17β-HSD type 2 in omental (OM) vs. subcutaneous (SC) adipose tissues of men. Formation of 4-dione from testosterone was significantly higher in homogenates ($p \leq 0.001$) and explants ($p \leq 0.01$) of OM than SC tissue. Microscopy analyses and biochemical assays in cell fractions localized the enzyme in the vasculature/endothelial cells of adipose tissues. Conversion of testosterone to 4-dione was weakly detected in most OM and/or SC preadipocyte cultures. Positive correlations were found between 17β-HSD type 2 activity in whole tissue and BMI or SC adipocyte diameter. We conclude that conversion of testosterone to 4-dione detected in abdominal adipose tissue is caused by 17β-HSD type 2 which is localized in the vasculature of the adipose compartment.

Keywords: 17β-HSD, 17β-HSD type 2, testosterone, adipose tissue

1. INTRODUCTION

Androgens likely modulate body fat distribution in men and women [reviewed in (Blouin et al., 2009,Zerradi et al., 2014)]. Intra-abdominal fat accumulation is negatively correlated with circulating androgens in both sexes (Blouin et al., 2005,Cote et al., 2012) and testosterone replacement in men leads to lower waist circumference and improved metabolic profile (Haider et al., 2014). From the cellular standpoint, androgens inhibit preadipocyte differentiation (Blouin et al., 2008,Chazenbalk et al., 2013,Gupta et al., 2008). Testosterone also has a negative effect on mitochondrial biogenesis through promoting a decrease in mitochondrial mass in 3T3-L1 adipocytes (Capllonch-Amer et al., 2014). Lipolysis is increased in cultured adipocytes after androgen treatment [Reviewed in (Blouin et al., 2008)]. Testosterone also induces a decrease in adiponectin receptor and adiponectin expression which is consistent with an inhibitory effect on lipid accumulation and fat cell differentiation (Capllonch-Amer et al., 2014).

17β-hydroxysteroid dehydrogenases (17β-HSDs) play an important role in the biological activity of steroid hormones such as estrogens and androgens by catalyzing the reduction of 17-ketosteroids or the oxidation of 17β-hydroxysteroids with NAD(P)H or $NAD(P)^+$ as cofactor, respectively (Luu-The, 2001). Enzyme activities associated with the various 17β-HSD isoforms are widespread in human tissues, not only in classic steroidogenic tissues such as the testis, ovary, and placenta, but also in a large number of peripheral sites including adipose tissue [reviewed in (Lin et al., 2013,Tchernof et al., 2014)].

Among 17β-HSD isoenzymes, 17β-HSD type 2 is a trans-membrane protein which has an unknown 3D-structure. It catalyzes the conversion of active 17β-hydroxysteroids into less active 17-ketosteroids with NAD+ as cofactor, which decreases tissue levels of active estrogens and androgens (Wetzel et al., 2011). Specifically, it is responsible for the conversion of testosterone to androstenedione (4-dione), of estradiol (E_2) to estrone (E_1) and of 20α-dihydroprogesterone to progesterone (Wu et al., 1993). The enzyme also exhibits 3β-HSD activity in intact cells and homogenates of transfected HEK 293 cells (Suzuki et al., 2000). 17β-HSD type 2 is expressed in liver, placenta, endometrium and small intestine. It may be involved in maintaining the level of progesterone in pregnancy by inactivating androgens and estrogens in the placenta (Wu et al., 1993). The enzyme also likely serves as a barrier that lowers E_2 secretion rates toward the foetal blood circulation (Drolet et al., 2007).

Little data are available on 17β-HSD type 2 in human abdominal adipose tissues. We have initially shown that 17β-HSD type 2 mRNA is more strongly expressed in omental (OM) adipose tissue than in subcutaneous (SC) adipose tissue of women (Blouin et al., 2009). Our objective was to evaluate the rate of testosterone conversion to 4-dione as well as expression and localization of 17β-HSD type 2 in human OM vs. SC adipose tissues obtained from male subjects at the time of surgery. We hypothesized that the conversion of testosterone to 4-dione is present in OM and SC adipose tissues in men and that 17β-HSD type 2 is responsible for this activity.

2. MATERIALS AND METHODS

2.1. Subjects

The study sample included obese and non-obese men recruited through the elective general surgery schedule of the CHU de Quebec Medical Center (Quebec City, Canada) and severely obese men undergoing bariatric surgery at the Quebec Heart and Lung Institute (Quebec City, Canada). The project was approved by the ethics committees of both institutions. All subjects provided written informed consent.

2.2. Adipose tissue sampling, preadipocyte isolation and differentiation

During the surgical procedure, adipose tissue samples were collected at the site of the surgical incision (lower abdomen, SC adipose tissue) and at the greater omentum (OM adipose tissue) and immediately carried to the laboratory. A portion of the sample was used for tissue explants, another was frozen for gene expression or preparation of homogenates and finally, a portion was used for isolation of preadipocytes. Samples were digested for 45 min at 37°C using type I collagenase in Krebs-Ringer-Henseleit buffer supplemented with 0.1 mg/ml ascorbic acid, 5 mM glucose, 0.1 μM adenosine, and 4% bovine serum albumin (BSA) according to a modified version of the Rodbell method (Rodbell, 1964). After tissue digestion, the cell suspension was filtered through nylon mesh and floating adipocytes were washed three times with Krebs-Ringer-Henseleit buffer. Preadipocytes were isolated from the stromal-vascular fraction using a modification of the Van Harmelen method (Van Harmelen et al., 2004). Briefly, the residual buffer, which contained the stromal-vascular fraction, was centrifuged and the pellet was washed in DMEM/F12. Preadipocytes were then filtered through a 140 μm nylon mesh and placed in

culture plates at 37°C under 5% CO_2 atmosphere. Cells were maintained in DMEM/F12 supplemented with 2.5% fetal bovine serum, 10 ng/ml epidermal growth factor, 1 ng/ml fibroblast growth factor, 6 μM insulin, 2.5 μg/ml amphotericin B and 50 μg/ml gentamicin. Medium was changed every 2-3 days. Differentiation of fully confluent preadipocyte cultures in 12-well plates was induced using commercial differentiation medium from Zen Bio (Durham, NC, USA), and followed for 14 days. Differentiation medium consisted of DMEM/F12 supplemented with a PPAR-γ agonist, insulin, dexamethasone and 3-isobutyl-1-methylxanthine.

2.3. Preparation of homogenates and cell/explant cultures

For homogenates, frozen adipose tissue samples (50 mg) were homogenized in sodium phosphate buffer, pH 7.4 (50 mM Na_2HPO_4, 50 mM NaH_2PO_4, 20% glycerol, 1 mM EDTA). The homogenates were centrifuged at 12000 rpm to remove the lipid layer. 800 μl of sodium phosphate buffer supplemented with 1 mM β-NAD and 0.144 μM ^{14}C-testosterone (American Radiolabeled Chemicals, St. Louis, MO, USA) were added to 200 μl of tissue homogenates followed by 24 h incubation at 37°C with shaking. For explants, fresh adipose tissue samples (100 mg) were cut into small pieces and incubated in M199 medium (30 mg tissue/mL) with ^{14}C-testosterone (0.1 μM) for 24 h at 37°C under a 5% CO_2 atmosphere. OM and SC preadipocyte cultures were treated with ^{14}C-testosterone (0.03 μM and 0.1 μM) and incubated for 24 h at 37°C under a 5% CO_2 atmosphere. For enzyme inhibition, preadipocyte cultures were treated with 10 μM 17β-HSD type 2 inhibitor EM-919 (Poirier et al., 2001). No toxicity of the inhibitor was detected on adipose tissue cultures using the Toxilight bioassay kit (Lonza, Allendale, NJ, USA). Fresh and frozen adipose tissue samples (130 mg) were homogenized in sodium phosphate

buffer, pH 7.4 and centrifuged at 12000 rpm to remove the lipid layer. 800 µl of sodium phosphate buffer supplemented with 2 mM β-NAD and 10 µM 17β-HSD type 2 inhibitor EM-919 were added to 200 µl of tissue homogenates followed by a 2 h pre-incubation at 37°C with shaking before addition of ^{14}C-testosterone (0.144 µM or 0.216 µM) for 24 h of incubation.

2.4. Steroid extraction and TLC measurements

Steroids from tissue homogenates, explants and preadipocyte culture media were extracted twice with 2 ml diethyl ether followed by drying under nitrogen gas. Dichloromethane was used to dissolve the steroids which were applied to silica gel thin layer chromatography (TLC) plates. Plates were developed in a sealed glass chamber containing 100 ml of toluene/acetone (4:1) and scanned on a Storm 860 PhosphorImager (GE Healthcare, Baie D'Urfe, QC, Canada). The inactivation rate of testosterone was expressed as androstenedione (4-dione) formation (pmol/µg protein/24 h) for homogenates and as (pmol/mg explants/24 h) for explants. Image J software was used for these calculations (NIH, Bethesda, MD, USA).

2.5. Measurement of mRNA expression by Real-time RT-PCR

Total RNA was extracted from whole OM and SC tissue, and from non-differentiated and differentiated preadipocyte cultures using the RNeasy lipid tissues mini kit and on-column DNase treatment (Qiagen, Hilden, DE) following the manufacturer's instructions. Total RNA quality was assessed on an Agilent BioAnalyzer (Agilent Technologies, Santa Clara, CA, USA). First-strand cDNA synthesis was accomplished using Superscript III RNase H-RT (Invitrogen Life

Technologies, Burlington, ON, CA), oligo-dT_{18}, random hexamers and purified with the PCR purification kit (Qiagen, Hilden, DE) was used to purify cDNA. cDNA corresponding to 20 ng of total RNA was used to perform fluorescent-based real-time RT-PCR quantification using the Light Cycler 480 (Roche Diagnostics, Mannheim, DE). The Light Cycler 480 SYBR Green I Master Reagent (Roche Diagnostics, Indianapolis, IN, USA) was used as recommended by the manufacturer. The conditions for PCR reactions were: 45 cycles, denaturation at 95°C for 10 sec, annealing at 57-60°C for 10 sec, elongation at 72°C for 14 sec and then 72-74°C for 5 sec (reading). A melting curve was generated to assess non-specific signal. PCR data were expressed as number of copies per microgram of total RNA (copies/µg total RNA). Calculation of the number of copies of each mRNA was performed according to (Luu-The et al., 2005) using second derivative method and a standard curve of Cp versus logarithm of the quantity. The standard curve was established using known amounts of purified PCR products (10, 10^2, 10^3, 10^4, 10^5 and 10^6 copies) and a LightCycler 480 v1.5 program provided by the manufacturer (Roche Diagnostics, Mannheim, DE). These measurements were performed by the CHU de Quebec Research Center (CHUL) Gene Expression Platform (Quebec, Canada) and were compliant with MIQE guidelines (Bustin et al., 2009). Primer sequences for 17β-HSD type 2 (NM_002153; forward: GCGCCTCTCGGTGCTCCAAATG, reverse: CGGCCATGCATTGTTTGTAGTCAGTCA and PPARγ (NM_138712; forward: GTCGGATCCACAAAAAAAGTAGAA, reverse: AGCGGGAAGGACTTTATGTATGA) were designed using Gene Tool (Biotools, Jupiter, FL, USA).

2.6. Western blotting

Following RNA extraction of whole OM and SC adipose tissues, one volume of ethanol was added to the lower phase of the trizol extraction. Trace DNA was removed by centrifugation at 2000×g for 2 min. The supernatant was vortexed with two volumes of isopropanol and incubated 10 min at room temperature. Proteins were precipitated by centrifugation at 5000×g for 10 min. The pellet was washed three times in 0.3 M guanidine in ethanol for 20 min followed by one wash with 100% ethanol. The pellet was then resuspended using heat (65°C) and sonication (10 s) cycles in 25 mM Tris, pH 7.4, 1.5 % SDS buffer containing protease inhibitors. A total of 30 µg of protein homogenate diluted in SDS buffer 4X (0.2 M Tris, pH 6.8, 8% SDS, 5 mM EDTA, 40% glycerol, 0.2 mM DTT) was heated at 95^{o}C for 3 min and separated on a 10% SDS-polyacrylamide gel. Proteins were transferred to nitrocellulose membranes (1 h at 100 V) and non-specific sites were blocked with 5% non-fat milk diluted in 1X TBS (10 mM Tris, pH 8.0, 150 mM NaCl, 0.05% Tween 20) for 1 h at room temperature. Membranes were then incubated overnight at 4^{o}C with rabbit primary antibody against 17β-HSD type 2 protein (kindly provided by Dr Yves Tremblay, CHU de Québec-Université Laval, Québec, Canada) and β-tubulin (Cell Signaling Technology, Danvers, MA, USA) as loading control. Membranes were washed and incubated 1 h with anti-rabbit immunoglobulin G conjugated to horseradish peroxidase (Jackson Immunoresearch Laboratories, West Grove, PA, USA). Finally, membranes were washed and proteins were visualized by chemiluminescence (Western Lightning Plus-ECL, Perkin Elmer, MA, USA). Densitometric analysis was performed with Image J (NIH, Bethesda, MD, USA).

2.7. Immunohistochemistry

Paraffin sections (5 mm-thick) were deparaffinized, hydrated, and treated with 3% H_2O_2 in methanol for 20 min. The sections were then incubated overnight at 4°C with 17β-HSD type 2 antibody [generated from New Zealand rabbits previously injected with the purified 17β-HSD type 2 protein as described in (Han et al., 2008)] with a dilution of 1:250. A commercial detection system kit (Covance Research Products Inc, Denham, MA, USA) using the streptavidin-biotin amplification method was used. Finally, the antigen-antibody complex was visualized with a solution of phosphate buffer saline (PBS) 1X containing 20 mg/100ml of 3,3-diaminobenzidine and 3% H_2O_2. Sections were lightly counterstained with hematoxylin. Control experiments were performed on adjacent sections using commercial normal rabbit serum (NRS) (1:250) instead of the primary antibody.

2.8. HAMEC Cultures

Human Adipose Microvascular Endothelial Cells (HAMEC) were purchased from Sciencell Research Laboratories (Carlsbad, CA). Cells were cultured following the manufacturer's instructions. To measure 17β-HSD type 2 specific activity, HAMEC cultures were pretreated with 10 μM of EM-919 inhibitor or vehicle and then with 0.03 μM ^{14}C-testosterone for 24 h at 37°C under a 5% CO2 atmosphere. Steroids from the culture media were extracted with diethyl ether and resolved on TLC as described above. The results were expressed as 4-dione formation (pmol/μg protein/24h). Total mRNA expression of CD31 (NM_000442; forward: GGCAAACCCTTCTATCAAATGACCT, reverse: TTGGCTCTGTTGAAGGCTGTG) and 17β-HSD2 genes were measured in HAMEC cultures by Real-time RT-PCR using the same conditions as above. For immunohistochemical localization of 17β-HSD type 2 in HAMEC, the

cells were cultivated on microslides and fixed in 10% formalin for 12 min. As mentioned in the immunohistochemistry section, a rabbit antibody against human 17β-HSD type 2 (Han et al., 2008) was used with a dilution of 1:500 and revealed using a streptavidin-biotin amplification method (Covance Research Products Inc, Denham, MA, USA). Normal rabbit serum was used as negative control.

2.9. Tridimensional confocal imaging

Human fat samples (2 x 2 mm, obese male donor) were fixed in a 4% formaldehyde solution for 2 h followed by three washes of 15 min with PBS prior to storage at 4°C in PBS. To ensure diffusion of antibodies, fixed tissue samples were dehydrated in a methanol series (50% once and 100% twice, 15 min each), then incubated for 2 h in a slightly modified solution of Dent's fixative (1:3 DMSO:methanol) (Aubin et al., 2015,Dent et al., 1989). Samples were then incubated overnight at 4°C with a bleaching solution (1:4 30% hydrogen peroxide: Dent's fixative) (Aubin et al., 2015,Dent et al., 1989,Dickie et al., 2006). Before immunolabeling, samples were rehydrated with a 15 min wash of 50% methanol, followed by three 15 min washes in PBS. Samples were saturated with a solution of 1% w/v of BSA in PBS for 30 min, then incubated with both a sheep anti-human CD31 (R&D Systems, MN, USA, AF806) and a rabbit anti-human 17β-HSD type 2 antibody (Han et al., 2008) for 3 days at 4°C. Samples were washed three times in PBS then probed with a donkey anti-sheep IgG-coupled Alexa 633 (A-21100) and a donkey anti-rabbit IgG-coupled Alexa 488 (A-21206) secondary antibodies (Life Technologies, Burlington, ON, Canada) for 3 days at 4°C. Isotypic sheep (Millipore, Billerica, MA, USA) and rabbit (R&D Systems, Minneapolis, MN, USA) antibodies were used as negative controls.

Optical clearing was then performed by dehydrating the samples again in a methanol series (50% once and 100% twice, 30 min each), followed by a methyl salicylate (Sigma Aldrich, ON, Canada) series (33%, 66% and 100% twice, 30 min each), then mounted in 100% methyl salicylate between two glass coverslips separated with a silicone isolator. Images were acquired using an LSM 700 inverted confocal scanning microscope system (Carl Zeiss, ON, Canada) controlled by Zen 2010 Software. Samples were imaged with a Plan-Neoflur 10x/0.3 or a Plan-Apochromat 20x/0.75 with a frame size of 1024 x 1024 pixels. 3D representations of the vascular network were created with Imaris 7.0.0 software (Bitplane, CT, USA).

2.10. Statistical analyses

Student's paired *t*-tests were performed to assess the depot difference in 17β-HSD type 2 activity in tissues homogenates and explants. These tests were also used to examine the difference in mRNA expression of 17β-HSD type 2 in whole adipose tissue and protein abundance in OM vs. SC adipose tissues. The difference in mRNA expression of 17β-HSD type 2 of non-differentiated and differentiated preadipocytes was assessed by repeated measures analysis of variance. Pearson correlations were computed to assess correlations between 17β-HSD type 2 activity in each fat depot and body mass index (BMI) or subcutaneous adipocyte diameter. Log_{10} transformation was used to normalize non-normally distributed variables. All data are presented as mean ± SEM. Statistical analyses were performed using JMP software (SAS Institute, Cary, NC, USA).

3. RESULTS

The conversion rate of ^{14}C-testosterone to 4-dione was measured in adipose tissue homogenates in both OM and SC adipose tissues from men (n=17, age 48.4±9.8 years, range 32.1-66.4 and BMI 39.5±13.4 kg/m^2, range 24.0-59.0 kg/m^2) **(Figure 1A)**. We found higher 4-dione formation in OM than in SC tissue ($p \leq 0.001$). This finding was supported by higher conversion rate of ^{14}C-testosterone to 4-dione in OM vs SC whole tissue explants (n=6, $p \leq 0.01$) **(Figure 1B)**.

Figure 2A shows 17β-HSD type 2 mRNA expression levels in whole OM and SC adipose tissue samples (n=20). The results indicated higher 17β-HSD type 2 mRNA abundance in OM than in SC adipose tissue ($p \leq 0.05$). **Figure 2B** shows the quantification of 17β-HSD type 2 protein in OM and SC tissues by Western blot analysis (n=6). At the protein level, the trend for higher 17β-HSD type 2 protein in OM vs SC tissue did not reach statistical significance.

A specific 17β-HSD type 2 inhibitor (EM-919) was used to confirm that this enzyme is responsible for testosterone inactivation in human OM and SC adipose tissues. **Figure 3A** shows the rates of 4-dione formation in OM (n=7) and SC (n=7) adipose tissue homogenates with and without 10 μM of EM-919 inhibitor. The results indicated a significantly lower 4-dione formation rate after exposure to the inhibitor in OM samples (inhibition of 56.3%, $p \leq 0.01$). Percent inhibition was non-significant in SC tissue homogenates (6.3%). To increase the assay sensitivity in SC tissue, the same experiment was done in SC tissue homogenates (n=7) with higher testosterone concentration (0.216 μM), with or without 10 μM EM-919 **(Figure 3B)**. We detected a significant decrease in 4-dione formation in these conditions (32.7% inhibition, $p < 0.001$).

We measured mRNA expression of 17β-HSD type 2 in preadipocyte cultures before and after induction of differentiation (14 days). As expected, PPARγ mRNA expression was higher after differentiation in both OM and SC preadipocyte cultures and a much higher induction was noted in SC cells ($p \leq 0.01$ for all) (**Figure 4A)**. The mRNA abundance of 17β-HSD type 2 mRNA was very low in these cultures but there was a trend for increased 17β-HSD type 2 mRNA expression after induction of differentiation ($p=0.06$) with a significant depot difference ($p=0.04$) and a significant time*depot interaction ($p=0.02$) (**Figure 4B)**.

Immunohistochemistry was used to establish 17β-HSD type 2 localization in human OM and SC adipose tissues by using a specific 17β-HSD type 2 antibody (**Figure 5)**. 17β-HSD type 2 was detected in the blood vessels of both OM and SC adipose tissues. We did not clearly detect the enzyme in adipocytes in the patients tested. To confirm this finding, we examined activity, expression and cellular localization of 17β-HSD type 2 in HAMEC cultures **(Figure 6)**. We measured a high rate of testosterone conversion into 4-dione which was strongly inhibited by EM-919 ($p<0.05$, 64% inhibition) **(Figure 6A)**. We also examined expression of 17β-HSD type 2 mRNA, as well as that of CD31, used as positive control. As expected, CD31 mRNA abundance was very high in these endothelial cells. Messenger RNA expression of 17β-HSD type 2 was also high **(Figure 6B)**. Immunohistochemical analysis positively identified 17β-HSD type 2 in HAMEC, with subcellular localization appearing more specifically in the endoplasmic reticulum of these cells **(Figure 6E and F)**.

We further investigated the localization of 17β-HSD type 2 using a tridimensional confocal imaging technique in fixed, native omental adipose tissue **(Figure 7)**. We used CD31 as a vascular cell marker. Clear co-localization of the 17β-HSD type 2 and CD31 proteins was found in the adipose tissue vasculature **(Figure 7C)**.

We investigated the correlation between conversion rates of testosterone to 4-dione in whole tissue homogenates from each compartment and body mass index (BMI) or adipocyte diameter. **Figure 8** shows a positive correlation between BMI and 17β-HSD type 2 activity in OM and SC tissues. A significant positive correlation between SC 17β-HSD type 2 activity and SC adipocyte diameter was also found. No correlation was found between OM 17β-HSD type 2 activity and OM adipocyte diameter.

When investigating whether 17β-HSD type 2 activity was present in cultures of isolated preadipocytes, little or no conversion of testosterone to 4-dione was detected in the vast majority of cultures upon treatment of with 0.03 μM ^{14}C-testosterone. In only a few exceptions, significant activity was detected. This activity was inhibited by EM-919 (**Figure 9)** and did not correlate with expression of endothelial cell marker CD31 (not shown).

4. DISCUSSION

We hypothesized that the conversion of testosterone to androstenedione (4-dione) can be detected in omental (OM) and subcutaneous (SC) adipose tissues of men and that 17β-HSD type 2 is responsible for this action. We found higher activity of 17β-HSD type 2 in human OM than SC adipose tissue homogenates and explants. We also localized the enzyme in the blood vessels of these tissue compartments. This is the first study to describe activity and localization of oxidative 17β-HSD type 2 in human abdominal adipose tissues. These findings add to the complexity of steroid conversions which may take place in the various cell types of adipose tissue and possibly affect local availability of active hormones.

The specific inhibitor of 17β-HSD-2, EM-919, is a weak estrogen spiro-δ-lactone, which has a C18-steroid nucleus. It has been proposed as a good inhibitor for oxidase activity of 17β-HSD type 2 with 62-66% inhibition rates (Poirier et al., 2001). Our experiments demonstrate that 17β-HSD type 2 is the isoenzyme responsible for the conversion of testosterone into 4-dione in human adipose tissues. The inhibition rates were 56.3% and 32.7% in OM and SC tissue homogenates respectively. They were comparable with previously reported values, and virtually all the activity in OM tissues was abolished by EM-919. Because activity was lower in SC tissue, increased sensitivity of the assay was required to detect significant inhibition in this compartment.

As mentioned, the rates of 4-dione formation were higher in OM than in SC adipose tissue in both homogenates and tissue explants. Messenger RNA expression of 17β-HSD type 2 was also higher in whole OM adipose tissue than in the SC compartment. These results are consistent with

previous studies (Blouin et al., 2009) in which we had reported that 17β-HSD type 2 mRNA expression was higher in OM than in SC adipose tissue of women. Only a trend for a depot difference was found at the protein level. This lack of statistical difference in the face of clearly higher activity in OM vs. SC tissues may be due to the smaller number of patients tested, the lower sensitivity of the western blot measurement and the high BMI of the donors for this experiment. Given that the enzyme appears to be localized in the blood vessels, we suggest that the depot difference in expression and activity may be due to the fact that OM adipose tissue is more vascularized than SC adipose tissue (Ibrahim, 2010).

Regarding cellular localization, our results clearly indicate that 17β-HSD type 2 is located in the vasculature of adipose tissue, more specifically in the endoplasmic reticulum of CD31-positive endothelial cells. Other studies indicated that 17β-HSD type 2 mRNA was detected in endometrial tissue (Casey et al., 1994), placenta, human fetal liver, gastrointestinal tract and urinary tract at 20 weeks of gestation. Moreover 17β-HSD type 2 immunoreactive protein was detected in surface epithelial cells of the stomach, small intestine, colon, hepatocytes and renal medulla (Takeyama et al., 2000). Consistent with our findings, 17β-HSD type 2 mRNA and activity were high in endothelial cell cultures from umbilical artery (HUAEC) and vein (HUVEC). In arteries, the higher level of 17β-HSD type 2 activity was comparable to that of the placenta, which suggested the presence of an expression gradient (Simard et al., 2011). Our results are consistent with those of Wu et al. (Wu et al., 1993) who reported that the 17β-HSD type 2 protein contains a carboxyl-terminal endoplasmic reticulum retention motif suggesting association to the endoplasmic reticulum membrane.

The physiological significance of the presence of 17β-HSD type 2 in the vasculature of adipose tissue remains to be established. Our results are consistent with those of Boulton et al., (Boulton et al., 1992) who studied the interconversion of steroid hormones in human adipose tissue *in vivo* through measurement of arteriovenous concentration differences. They found that testosterone was removed from plasma during passage through adipose tissue and that removal rates correlated with the arterial testosterone concentration. We can speculate that the conversion of active testosterone into inactive 4-dione via 17β-HSD type 2 in the vasculature of human abdominal adipose tissue may possibly affect the availability of testosterone and its impact on adipose tissue function and metabolism. This may include influence on body fat distribution, inhibition of preadipocyte differentiation (Blouin et al., 2010,Chazenbalk et al., 2013), and stimulation of lipolysis (Blouin et al., 2008). The depot-specific impact of our findings is difficult to assess. Blood flow in adipose tissue is tightly regulated and further studies are needed to assess the impact of 17β-HSD type 2 on adipocyte function. The presence of other 17β-HSD isoenzymes identified in adipose tissue [reviewed in Tchernof et al., 2014)], including 17β-HSD types 3 and 5 must also be considered. These enzymes predominantly catalyze the reaction opposite to that of 17β-HSD-2, that is, the conversion of 4-dione to testosterone. They have expression and activity patterns that are quite distinct from that of the type 2 isoenzyme. They are predominantly expressed in the preadipocyte/adipocyte fraction, and the type 5 isoenzyme shows opposite depot differences, with robust induction through the process of preadipocyte differentiation. Collectively, these findings illustrate the complexity of androgen dynamics in the various cell compartments of adipose tissues.

We found positive correlations between 17β-HSD type 2 activity in OM and SC adipose tissues and body mass index (BMI). The correlation was also positive between 17β-HSD type 2 activity in SC adipose tissue samples and SC adipocyte diameter. We speculate that these correlations may possibly be due to the presence of 17β-HSD type 2 in the blood vessels of adipose tissue. Vascularization increases with adipogenesis and adipose tissue growth (Nishimura et al., 2007). However, other studies reported that decreases in the capillary density occurs in overweight and obese subjects as seen with decreases in adipose tissue pO_2 (Pasarica et al., 2009) and suggested that lower adipose tissue perfusion is a common characteristic of obesity (Hosogai et al., 2007). Whether activity increases in obesity are due to increases in vascularization or to specific up-regulation of the enzyme in endothelial cells remains to be determined.

For the vast majority of patients, activity of 17β-HSD type 2 was very low in SC and OM preadipocyte cultures, which is consistent with a primary localization of the enzyme in endothelial cells. In only a few exceptions, significant activity was detected in isolated preadipocytes upon incubation with a physiological dose of ^{14}C-testosterone. As shown in Figure 9, this activity was inhibited by EM-919, suggesting that 17β-HSD-2 was responsible for it. Yet, it did not correlate with expression levels of CD31, indirectly suggesting that it may not simply reflect endothelial cell contamination of the culture. These intriguing findings suggest that there is inter-individual variation in 17β-HSD type 2 activity of the preadipocyte compartment. Further studies are needed to establish the prevalence, origins and physiological significance of such divergent 17β-HSD activity pattern in some individuals.

In summary, we demonstrated that testosterone can be converted to 4-dione in human abdominal adipose tissues and that 17β-HSD type 2, which appears to be primarily localized in the vasculature, is responsible for this activity.

FUNDING

This study was funded by the Canadian Institute of Health Research to A.T. (MOP-130313). M.F.M. was funded by the Egyptian ministry of higher education (Cultural Affairs & Missions Sector). The confocal imaging system was obtained through the Fonds des leaders program from Canada Foundation for Innovation (CFI) to J.F.

CONFLICT OF INTEREST

The authors have no conflict of interest to disclose.

ACKNOWLEDGEMENTS

We acknowledge the collaboration of study participants. We would like to acknowledge the contribution of nurses and team members, of Johanne Ouellet and the surgery teams (Laurent Biertho, Simon Marceau, Frédéric-Simon Hould, Picard Marceau, Simon Biron, Odette Lescelleur, Jean Péloquin and Guy Roy).

REFERENCES

Aubin, K., Vincent, C., Proulx, M., Mayrand, D. and Fradette, J., 2015. Creating capillary networks within human engineered tissues: impact of adipocytes and their secretory products, Acta Biomater. 11, 333-45.

Blouin, K., Boivin, A. and Tchernof, A., 2008. Androgens and body fat distribution, J Steroid Biochem Mol Biol. 108, 272-80.

Blouin, K., Despres, J.P., Couillard, C., Tremblay, A., Prud'homme, D., Bouchard, C. and Tchernof, A., 2005. Contribution of age and declining androgen levels to features of the metabolic syndrome in men, Metabolism. 54, 1034-40.

Blouin, K., Nadeau, M., Mailloux, J., Daris, M., Lebel, S., Luu-The, V. and Tchernof, A., 2009. Pathways of adipose tissue androgen metabolism in women: depot differences and modulation by adipogenesis, Am J Physiol Endocrinol Metab. 296, E244-55.

Blouin, K., Nadeau, M., Perreault, M., Veilleux, A., Drolet, R., Marceau, P., Mailloux, J., Luu-The, V. and Tchernof, A., 2010. Effects of androgens on adipocyte differentiation and adipose tissue explant metabolism in men and women, Clin Endocrinol (Oxf). 72, 176-88.

Blouin, K., Veilleux, A., Luu-The, V. and Tchernof, A., 2009. Androgen metabolism in adipose tissue: recent advances, Mol Cell Endocrinol. 301, 97-103.

Boulton, K.L., Hudson, D.U., Coppack, S.W. and Frayn, K.N., 1992. Steroid hormone interconversions in human adipose tissue in vivo, Metabolism. 41, 556-9.

Bustin, S.A., Benes, V., Garson, J.A., Hellemans, J., Huggett, J., Kubista, M., Mueller, R., Nolan, T., Pfaffl, M.W., Shipley, G.L., Vandesompele, J. and Wittwer, C.T., 2009. The MIQE guidelines: minimum information for publication of quantitative real-time PCR experiments, Clin Chem. 55, 611-22.

Capllonch-Amer, G., Llado, I., Proenza, A.M., Garcia-Palmer, F.J. and Gianotti, M., 2014. Opposite effects of 17-beta estradiol and testosterone on mitochondrial biogenesis and adiponectin synthesis in white adipocytes, J Mol Endocrinol. 52, 203-14.

Casey, M.L., MacDonald, P.C. and Andersson, S., 1994. 17 beta-Hydroxysteroid dehydrogenase type 2: chromosomal assignment and progestin regulation of gene expression in human endometrium, J Clin Invest. 94, 2135-41.

Chazenbalk, G., Singh, P., Irge, D., Shah, A., Abbott, D.H. and Dumesic, D.A., 2013. Androgens inhibit adipogenesis during human adipose stem cell commitment to preadipocyte formation, Steroids. 78, 920-6.

Cote, J.A., Lessard, J., Mailloux, J., Laberge, P., Rheaume, C. and Tchernof, A., 2012. Circulating 5alpha-dihydrotestosterone, abdominal obesity and adipocyte characteristics in women, Horm Mol Biol Clin Investig. 12, 391-400.

Dent, J.A., Polson, A.G. and Klymkowsky, M.W., 1989. A whole-mount immunocytochemical analysis of the expression of the intermediate filament protein vimentin in Xenopus, Development. 105, 61-74.

Dickie, R., Bachoo, R.M., Rupnick, M.A., Dallabrida, S.M., Deloid, G.M., Lai, J., Depinho, R.A. and Rogers, R.A., 2006. Three-dimensional visualization of microvessel architecture of whole-mount tissue by confocal microscopy, Microvasc Res. 72, 20-6.

Drolet, R., Simard, M., Plante, J., Laberge, P. and Tremblay, Y., 2007. Human type 2 17 beta-hydroxysteroid dehydrogenase mRNA and protein distribution in placental villi at mid and term pregnancy, Reprod Biol Endocrinol. 5, 30.

Gupta, V., Bhasin, S., Guo, W., Singh, R., Miki, R., Chauhan, P., Choong, K., Tchkonia, T., Lebrasseur, N.K., Flanagan, J.N., Hamilton, J.A., Viereck, J.C., Narula, N.S., Kirkland, J.L. and Jasuja, R., 2008. Effects of dihydrotestosterone on differentiation and proliferation of human mesenchymal stem cells and preadipocytes, Mol Cell Endocrinol. 296, 32-40.

Haider, A., Saad, F., Doros, G. and Gooren, L., 2014. Hypogonadal obese men with and without diabetes mellitus type 2 lose weight and show improvement in cardiovascular risk factors when treated with testosterone: an observational study, Obes Res Clin Pract. 8, e339-49.

Han, B., Li, S., Song, D., Poisson-Pare, D., Liu, G., Luu-The, V., Ouellet, J., Li, S., Labrie, F. and Pelletier, G., 2008. Expression of 17beta-hydroxysteroid dehydrogenase type 2 and type 5 in breast cancer and adjacent non-malignant tissue: a correlation to clinicopathological parameters, J Steroid Biochem Mol Biol. 112, 194-200.

Hosogai, N., Fukuhara, A., Oshima, K., Miyata, Y., Tanaka, S., Segawa, K., Furukawa, S., Tochino, Y., Komuro, R., Matsuda, M. and Shimomura, I., 2007. Adipose tissue hypoxia in obesity and its impact on adipocytokine dysregulation, Diabetes. 56, 901-11.

Ibrahim, M.M., 2010. Subcutaneous and visceral adipose tissue: structural and functional differences, Obes Rev. 11, 11-8.

Lin, S.X., Poirier, D. and Adamski, J., 2013. A challenge for medicinal chemistry by the 17beta-hydroxysteroid dehydrogenase superfamily: an integrated biological function and inhibition study, Curr Top Med Chem. 13, 1164-71.

Luu-The, V., 2001. Analysis and characteristics of multiple types of human 17beta-hydroxysteroid dehydrogenase, J Steroid Biochem Mol Biol. 76, 143-51.

Luu-The, V., Paquet, N., Calvo, E. and Cumps, J., 2005. Improved real-time RT-PCR method for high-throughput measurements using second derivative calculation and double correction, Biotechniques. 38, 287-93.

Nishimura, S., Manabe, I., Nagasaki, M., Hosoya, Y., Yamashita, H., Fujita, H., Ohsugi, M., Tobe, K., Kadowaki, T., Nagai, R. and Sugiura, S., 2007. Adipogenesis in obesity requires close interplay between differentiating adipocytes, stromal cells, and blood vessels, Diabetes. 56, 1517-26.

Pasarica, M., Sereda, O.R., Redman, L.M., Albarado, D.C., Hymel, D.T., Roan, L.E., Rood, J.C., Burk, D.H. and Smith, S.R., 2009. Reduced adipose tissue oxygenation in human obesity: evidence for rarefaction, macrophage chemotaxis, and inflammation without an angiogenic response, Diabetes. 58, 718-25.

Poirier, D., Bydal, P., Tremblay, M.R., Sam, K.M. and Luu-The, V., 2001. Inhibitors of type II 17beta-hydroxysteroid dehydrogenase, Mol Cell Endocrinol. 171, 119-28.

Rodbell, M., 1964. metabolism of isolated fat cells. i. effects of hormones on glucose metabolism and lipolysis, J Biol Chem. 239, 375-80.

Simard, M., Drolet, R., Blomquist, C.H. and Tremblay, Y., 2011. Human type 2 17beta-hydroxysteroid dehydrogenase in umbilical vein and artery endothelial cells: differential inactivation of sex steroids according to the vessel type, Endocrine. 40, 203-11.

Suzuki, T., Sasano, H., Andersson, S. and Mason, J.I., 2000. 3beta-hydroxysteroid dehydrogenase/delta5-->4-isomerase activity associated with the human 17beta-hydroxysteroid dehydrogenase type 2 isoform, J Clin Endocrinol Metab. 85, 3669-72.

Takeyama, J., Suzuki, T., Hirasawa, G., Muramatsu, Y., Nagura, H., Iinuma, K., Nakamura, J., Kimura, K.I., Yoshihama, M., Harada, N., Andersson, S. and Sasano, H., 2000. 17beta-hydroxysteroid dehydrogenase type 1 and 2 expression in the human fetus, J Clin Endocrinol Metab. 85, 410-6.

Tchernof, A., Mansour, M.F., Pelletier, M., Boulet, M.M., Nadeau, M. and Luu-The, V., 2014. Updated survey of the steroid-converting enzymes in human adipose tissues, J Steroid Biochem Mol Biol. 147c, 56-69.

Van Harmelen, V., Rohrig, K. and Hauner, H., 2004. Comparison of proliferation and differentiation capacity of human adipocyte precursor cells from the omental and subcutaneous adipose tissue depot of obese subjects, Metabolism. 53, 632-7.

Wetzel, M., Marchais-Oberwinkler, S. and Hartmann, R.W., 2011. 17beta-HSD2 inhibitors for the treatment of osteoporosis: Identification of a promising scaffold, Bioorg Med Chem. 19, 807-15.

Wu, L., Einstein, M., Geissler, W.M., Chan, H.K., Elliston, K.O. and Andersson, S., 1993. Expression cloning and characterization of human 17 beta-hydroxysteroid dehydrogenase type 2, a microsomal enzyme possessing 20 alpha-hydroxysteroid dehydrogenase activity, J Biol Chem. 268, 12964-9.

Zerradi, M., Dereumetz, J., Boulet, M.M. and Tchernof, A., 2014. Androgens, body fat Distribution and Adipogenesis, Current Obesity Reports. 3:396-403.

FIGURE LEGENDS

Figure 1. Androstenedione formation rates in adipose tissue homogenates and explant culture (A) Androstenedione formation rate in omental (OM) and subcutaneous (SC) adipose tissue homogenates following 24 h exposure to ^{14}C-testosterone (n=17). **(B)** Androstenedione formation rate in OM and SC tissue explants following 24 h exposure to ^{14}C-testosterone (n=6). Mean ± SEM are shown. **p≤0.01, ***p≤0.001.

Figure 2. 17β-HSD type 2 mRNA expression and protein quantification (A) 17β-HSD type 2 mRNA expression in whole omental (OM) and subcutaneous (SC) adipose tissue samples expressed as number of copies/µg total RNA (n=20) **(B)** 17β-HSD type 2 protein level relative to β-tubulin in whole OM and SC adipose tissue samples (n=6). Mean ± SEM are shown. *p≤0.05.

Figure 3. Androstenedione formation rates in OM and SC whole tissue homogenates with and without exposure to 10 µM EM-919. (A) Effect of EM-919 (EM) on the conversion of testosterone (0.144 µM) to androstenedione in OM (n=7) and SC (n=7) adipose tissue samples. Five patients included here were also among the n=17 described in Figure 1A and 2A **(B)** Effect of EM-919 (EM) on the conversion of testosterone (0.216 µM) to androstenedione in SC adipose tissue samples (n=7). Mean ± SEM are shown. **p≤0.01, ***p<0.001.

Figure 4. PPARγ and 17β-HSD type 2 mRNA expression in non-differentiated and differentiated primary preadipocyte cultures. PPARγ **(A)** and 17β-HSD type 2 **(B)** mRNA

expression were examined in OM (n=5) and SC (n=7) cells before and 14 days after induction of differentiation. Mean ± SEM are shown. **p≤0.01.

Figure 5. Immunohistochemical localization of 17β-HSD type 2 in OM and SC adipose tissues. (A) OM negative control, rabbit antiserum. **(B)** 17β-HSD type 2 antibody in OM adipose tissue. **(C)** SC negative control, rabbit antiserum. **(D)** 17β-HSD type 2 antibody in SC adipose tissue. Scale bar 20 μM.

Figure 6: Human Adipose Microvascular Endothelial Cells (HAMEC). (A) Androstenedione formation rate after 24h incubation with 0.03μM ^{14}C-testosterone and inhibition with EM-919 (EM). **(B)** mRNA expression level of CD31 and 17β-HSD type 2 expressed as number of copies/μg total RNA. Immunohistochemical localization of 17β-HSD type 2, **(C, D)** Rabbit antiserum, **(E, F)** 17β-HSD type 2. Scale bar 20 μm. Mean ± SEM are shown. *p<0.05.

Figure 7. Tridimensional confoncal imaging of **(A)** CD31 and **(B)** 17β-HSD type 2 expression in blood vessels of omental native human fat. **(C)** Merging of the labellings and **(D)** Isotype controls.

Figure 8. Pearson correlations between 17β-HSD type 2 activity and anthropometric measurements. Pearson correlations between 17β-HSD type 2 activity in omental (OM) or subcutaneous (SC) adipose tissue homogenates and body mass index (BMI) **(A, B)** or adipocyte diameter in the OM and SC compartments **(C, D)**.

Figure 9. Thin layer chromatography (TLC) image of steroids extracted from cultures of preadipocytes in a patient with little activity in SC and OM cells (A) and a patient with detectable activity in SC cells (B). Steroids were extracted from primary preadipocyte culture media of OM and SC cells after 24 h incubation with 0.03 μM ^{14}C-testosterone. Δ4: androstenedione, T: testosterone, Ctl: control, EM: EM-919, Std: standard.

FIGURES

Figure 1

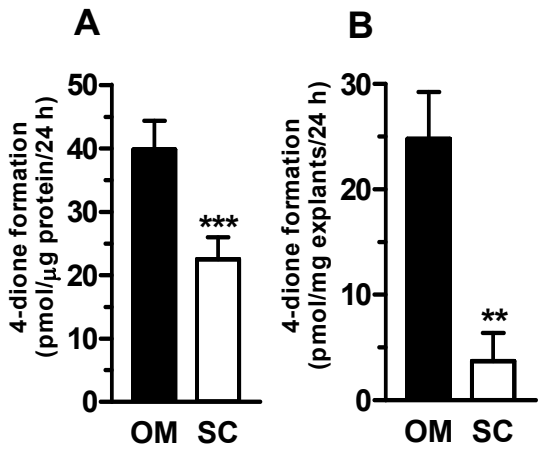

Figure 2

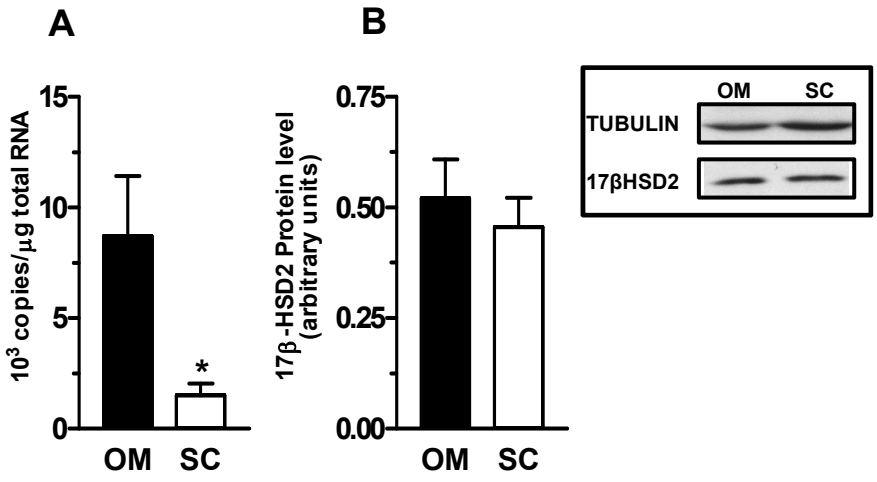
A
B
15
10
5
0
10^3 copies/μg total RNA
*
OM
SC
0.75
0.50
0.25
0.00
17β-HSD2 Protein level (arbitrary units)
OM
SC
TUBULIN
17βHSD2

Figure 3

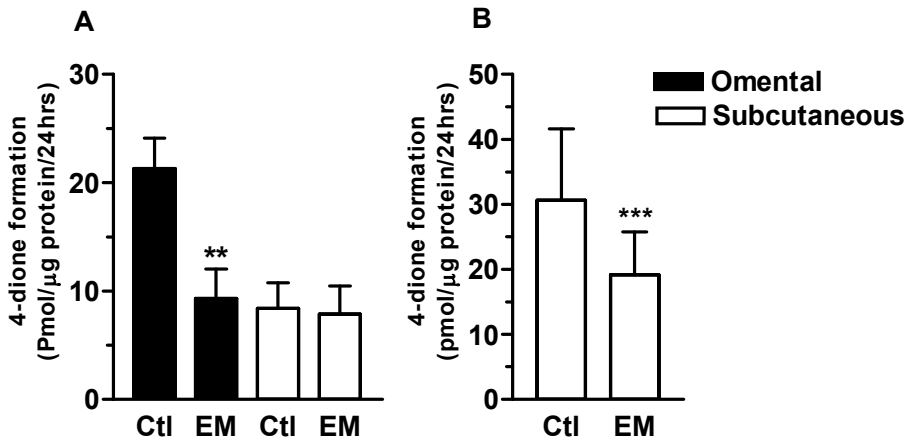
A
B
4-dione formation
(Pmol/µg protein/24hrs)
4-dione formation
(pmol/µg protein/24hrs)
30
20
10
0
50
40
30
20
10
0
**
***
Omental
Subcutaneous
Ctl
EM
Ctl
EM
Ctl
EM

Figure 4

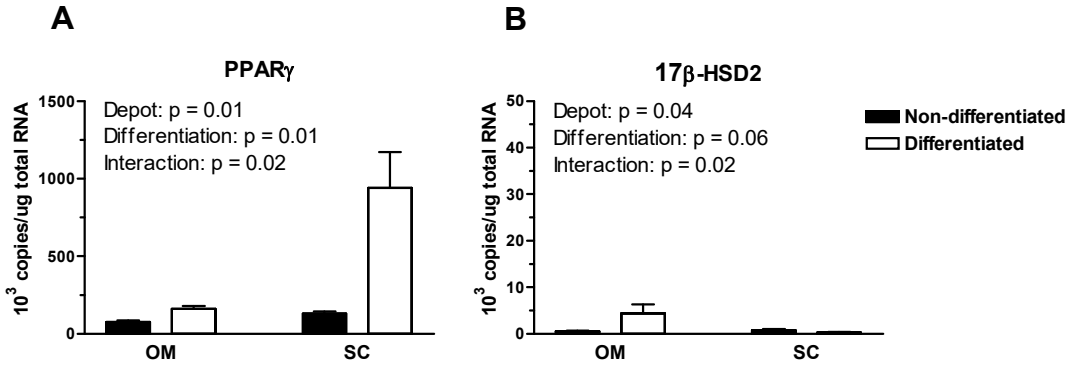
A
PPARγ
Depot: p = 0.01
Differentiation: p = 0.01
Interaction: p = 0.02
10^3 copies/ug total RNA
1500
1000
500
0
OM
SC
B
17β-HSD2
Depot: p = 0.04
Differentiation: p = 0.06
Interaction: p = 0.02
10^3 copies/ug total RNA
50
40
30
20
10
0
OM
SC
Non-differentiated
Differentiated

Figure 5

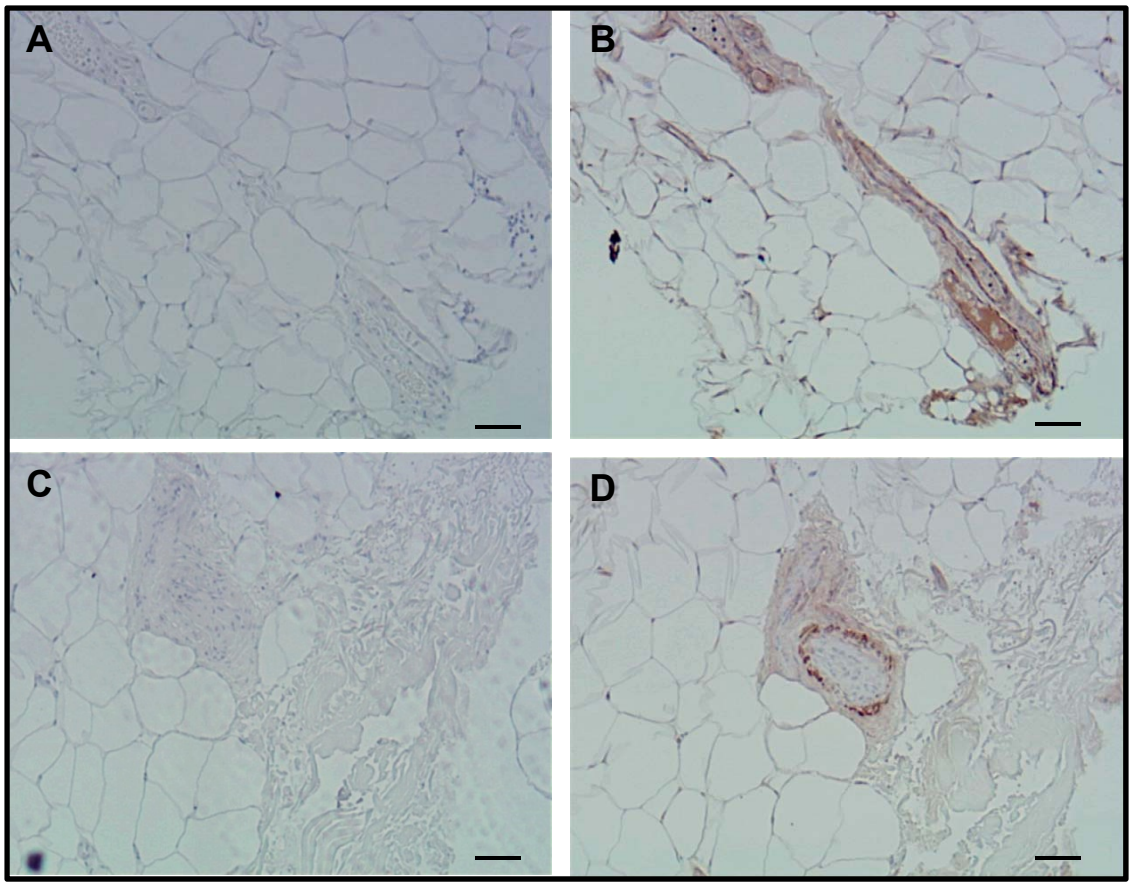

Figure 6

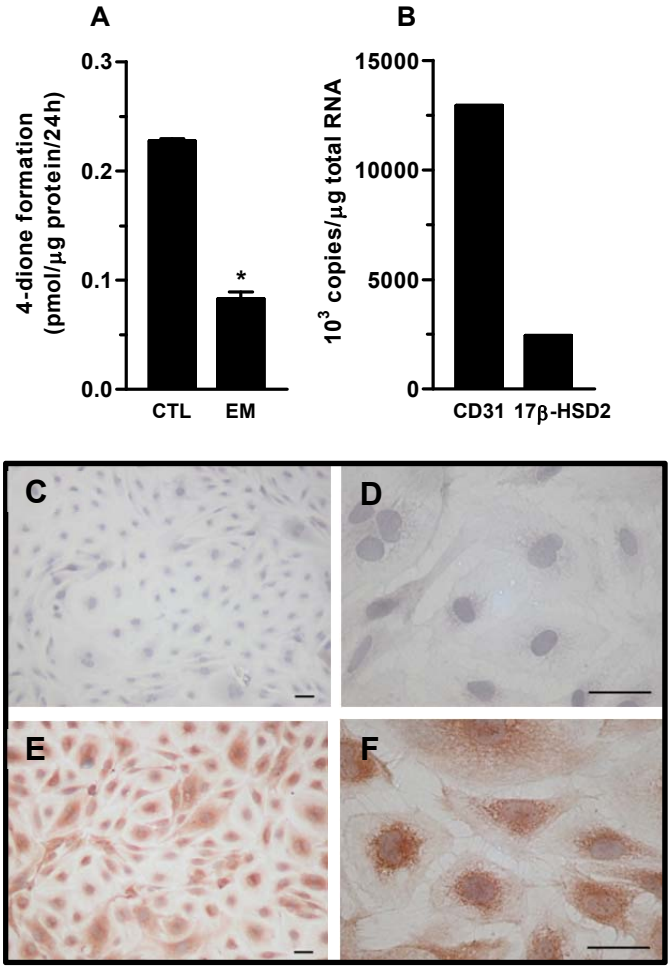
A
B
4-dione formation (pmol/µg protein/24h)
0.3
0.2
0.1
0.0
*
CTL
EM
10³ copies/µg total RNA
15000
10000
5000
0
CD31
17β-HSD2
C
D
E
F

Figure 7

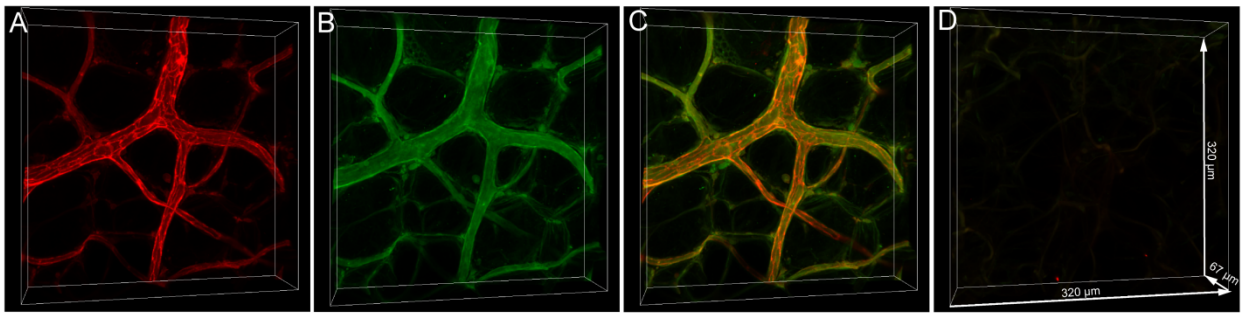

Figure 8

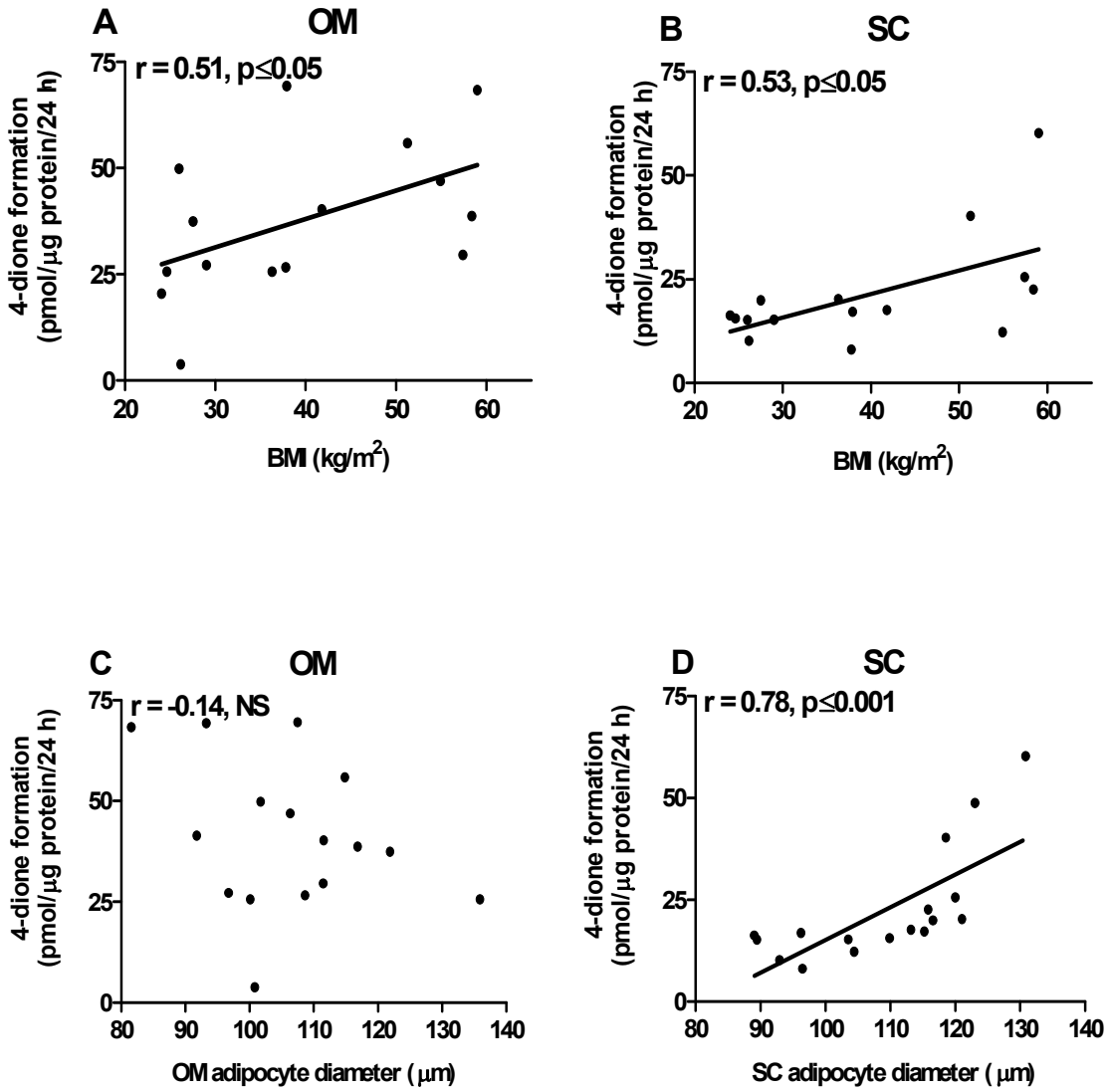
A
OM
r = 0.51, p≤0.05
4-dione formation (pmol/μg protein/24 h)
BMI (kg/m2)
B
SC
r = 0.53, p≤0.05
4-dione formation (pmol/μg protein/24 h)
BMI (kg/m2)
C
OM
r = -0.14, NS
4-dione formation (pmol/μg protein/24 h)
OM adipocyte diameter (μm)
D
SC
r = 0.78, p≤0.001
4-dione formation (pmol/μg protein/24 h)
SC adipocyte diameter (μm)

Figure 9